Two Novel Co(II) Coordination Polymers Based on 1,4-bis(3-pyridylaminomethyl)benzene as electrocatalysts for the oxygen evolution from water

Yun Gong, [a] **Zhi Hao,** [a] **Peng-Gang Jiang,** [a] **Jun-Liang Sun** [b] **and Jian-Hua Lin** [*a]

[a] *Department of Applied Chemistry, College of Chemistry and Chemical Engineering, Chongqing University, Chongqing 400030, P. R. China Tel: +86-023-65102316 E-mail: jhlin@cqu.edu.cn or jhlin@pku.edu.cn*

[b] *State Key Laboratory of Rare Earth Materials Chemistry and Applications, College of Chemistry and Molecular Engineering, Peking University, Beijing 100871, China*

## Determination of Faradaic Efficiency

Controlled potential electrolyses were conducted in a 30 mL aqueous solution buffered to neutral pH (0.2 M phosphate, pH 6.8) at an applied potential of □+1.4 V vs SCE (η = 0.81 V) for 2 hours. Assuming 100% Faradaic efficiency, the theoretical pH change over time can be calculated by the equation of pH = 14 + lg {Σ(It)/(FV)}, where I = current (A), t = time (s), F = Faraday constant (96485 C/mol), V = solution volume (0.03 L). [1] The generated O_2 volume during electrolysis was quantitatively and qualitatively analyzed by using a GC instrument (Shimadzu GC-8A) equipped with a 1 m column filled with Molecular Sieve 13X using He as the carrier gas and GC-MS instrument (Shimadzu GCMS-QP 1000EX), respectively. The theoretical (assuming 100% Faradic efficiency) O_2 volume is based on the amount of consumed charge during the course of electrolysis.

**Table S1** Selected bond lengths (Å) and angles (°) for complexes **1-2**

Complex 1

Co(1)-N(1)	2.105(14)	Co(2)-N(5)	2.019(14)
Co(3)-N(3)#3	2.074(12)	Co(1)-O(11)#1	2.006(15)
Co(2)-O(10)	2.141(15)	Co(3)-O(8)#2	2.121(13)
O(9)-Co(1)-O(1)	164.7(5)	O(6)-Co(2)-O(10)	86.2(6)
O(5)-Co(1)-O(9)	92.2(6)	O(7)-Co(3)-N(3)#3	105.9(5)
O(5)-Co(1)-N(1)	95.7(6)	O(1)-Co(1)-N(1)	89.8(5)

Complex 2

Co(1)-O(3)#4	2.062(6)	Co(1)-O(7)	2.140(6)
Co(1)-O(2)	2.160(7)	Co(1)-O(1)	2.230(6)
Co(1)-N(2)	2.185(8)	Co(1)-N(4)#3	2.190(8)
O(2)-Co(1)-O(1)	60.1(2)	O(3)#4-Co(1)-O(1)	164.0(2)
O(3)#4-Co(1)-N(4)#3	84.6(3)	N(4)#3-Co(1)-O(1)	93.6(3)
N(2)-Co(1)-O(1)	92.0(3)	N(2)-Co(1)-N(4)#3	173.8(3)
N(4)#5-Cd(1)-N(1)	173.89(16)	N(8)#5-Cd(2)-N(5)	175.40(17)

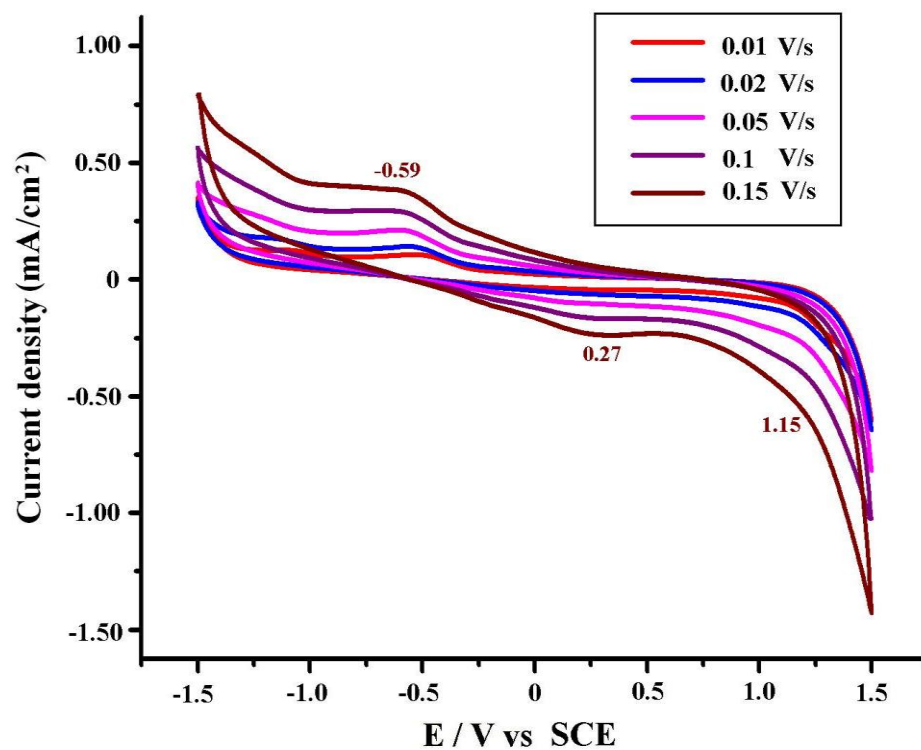Symmetry transformations used to generate equivalent atoms:

#1 -x+1,-y+2,-z+1   #2 -x+1,-y+1,-z   #3 -x+2,-y,-z   #4 x,y-1,z   #5 x,y+1,z
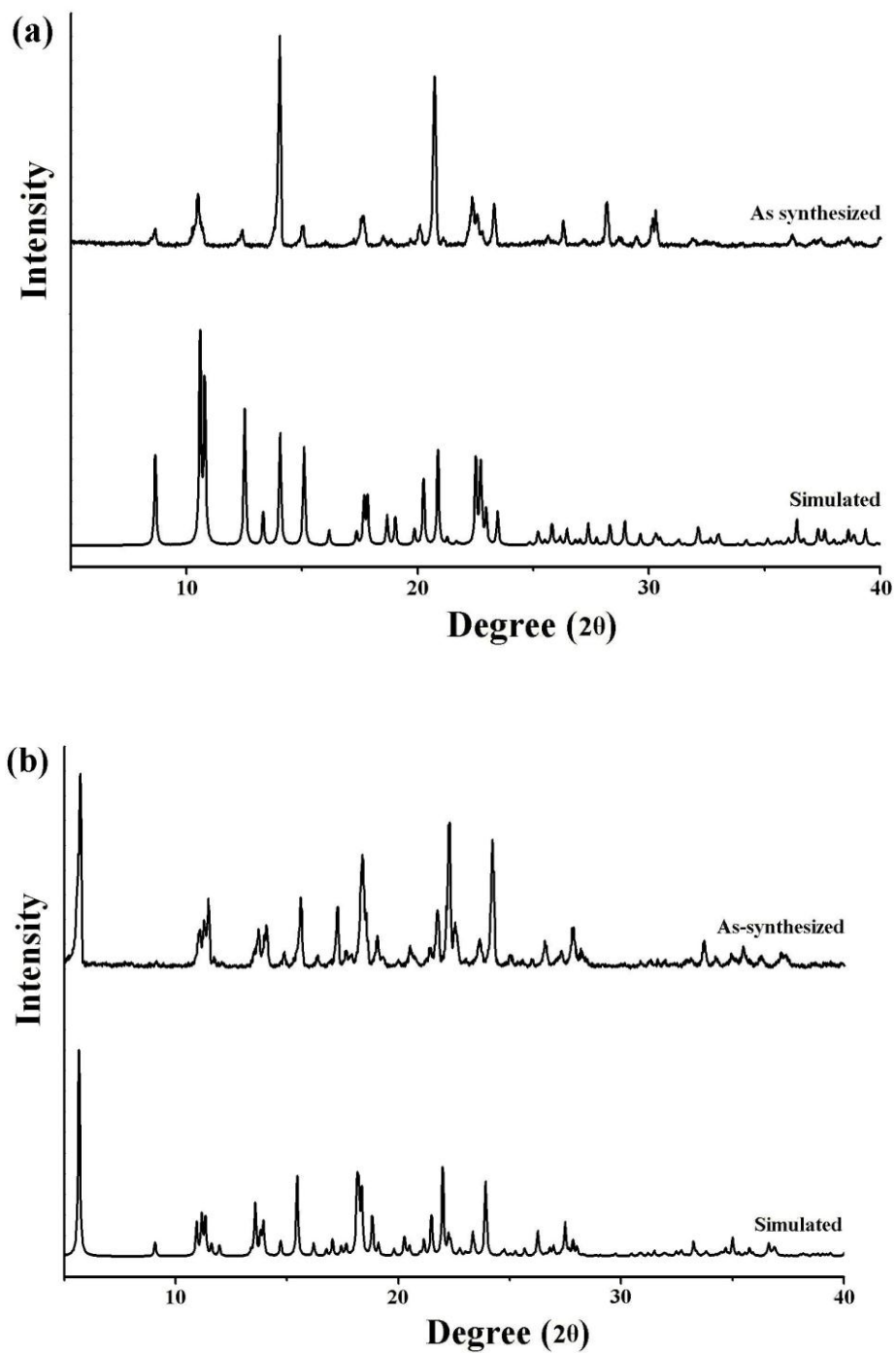
Fig.S1 The PXRD patterns of complexes **1 (a)** and **2 (b).**
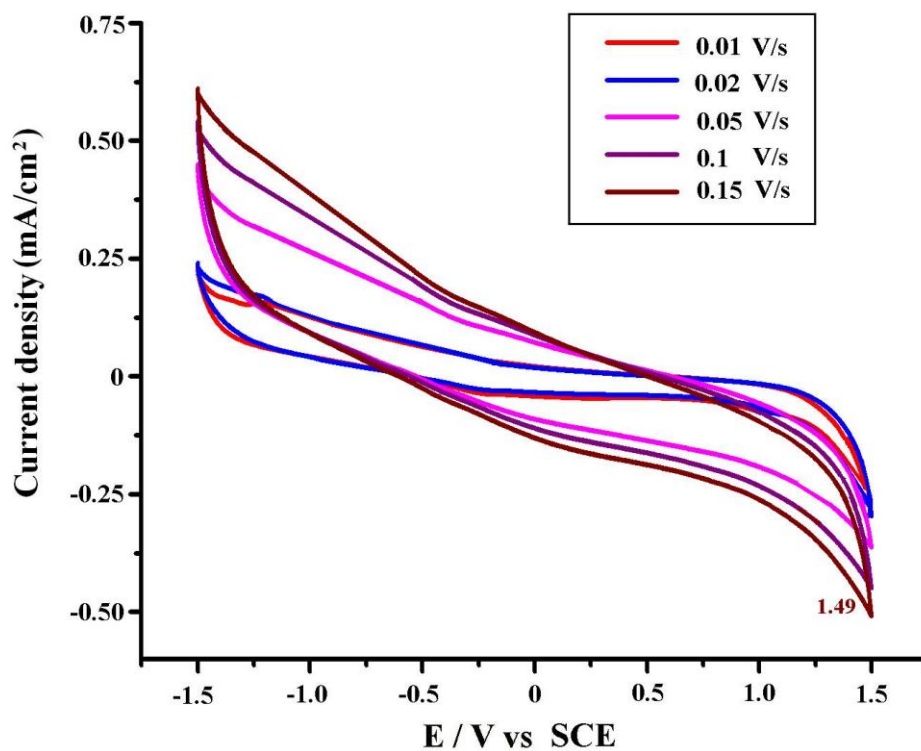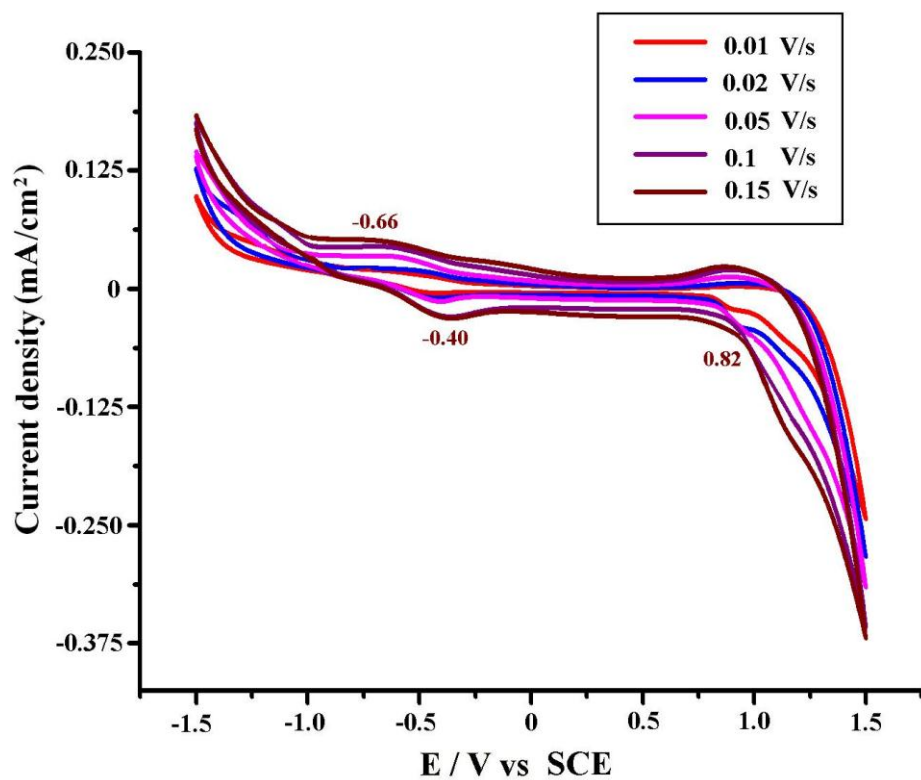
Fig. S2 Cyclic voltammograms of the bare **GCE** in an aqueous solution buffered to neutral pH (0.2 M phosphate, pH = 6.8) at different sweep rates.

Fig. S3 Cyclic voltammograms of the bare **GCE** in an aqueous solution buffered to neutral pH (0.2 M phosphate, pH = 6.8) containing 4 mg **H₂adip** at different sweep rates.
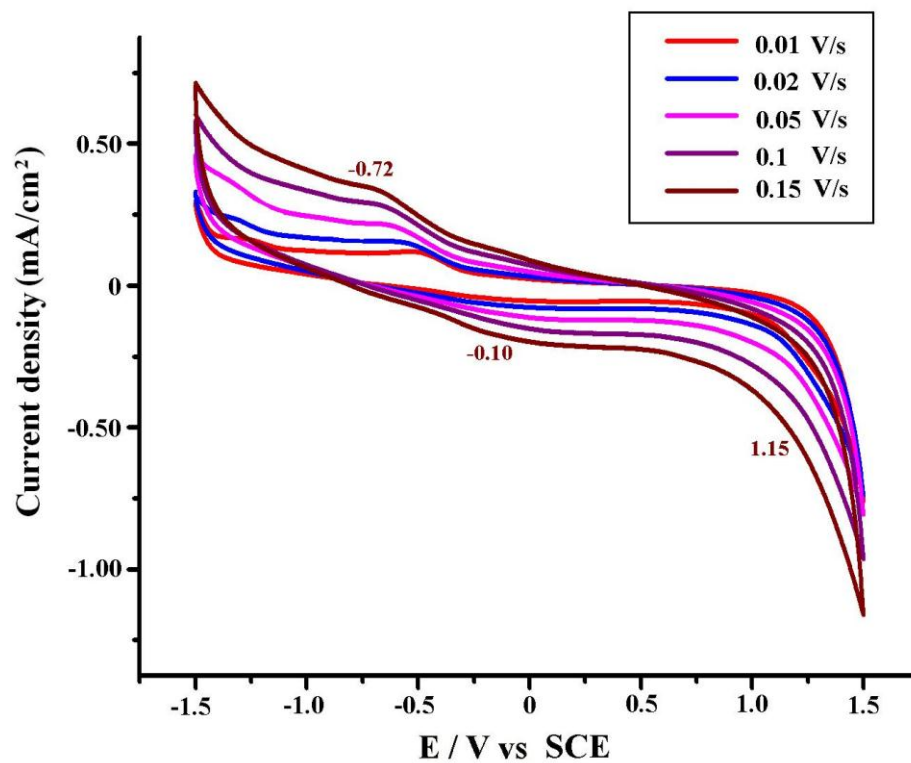
Fig. S4 Cyclic voltammograms of the bare **GCE** in an aqueous solution buffered to neutral pH (0.2 M phosphate, pH = 6.8) containing 4 mg **L** at different sweep rates.
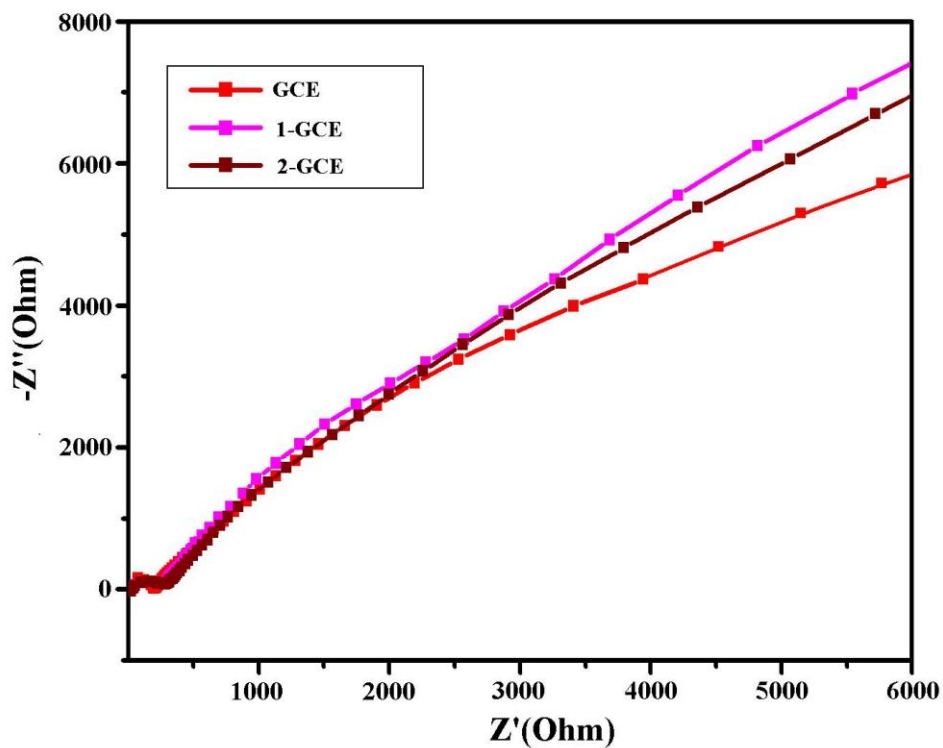
Fig. S5 Cyclic voltammograms of **1-GCE** in an aqueous solution buffered to neutral pH

(0.2 M phosphate, pH = 6.8) at different sweep rates.
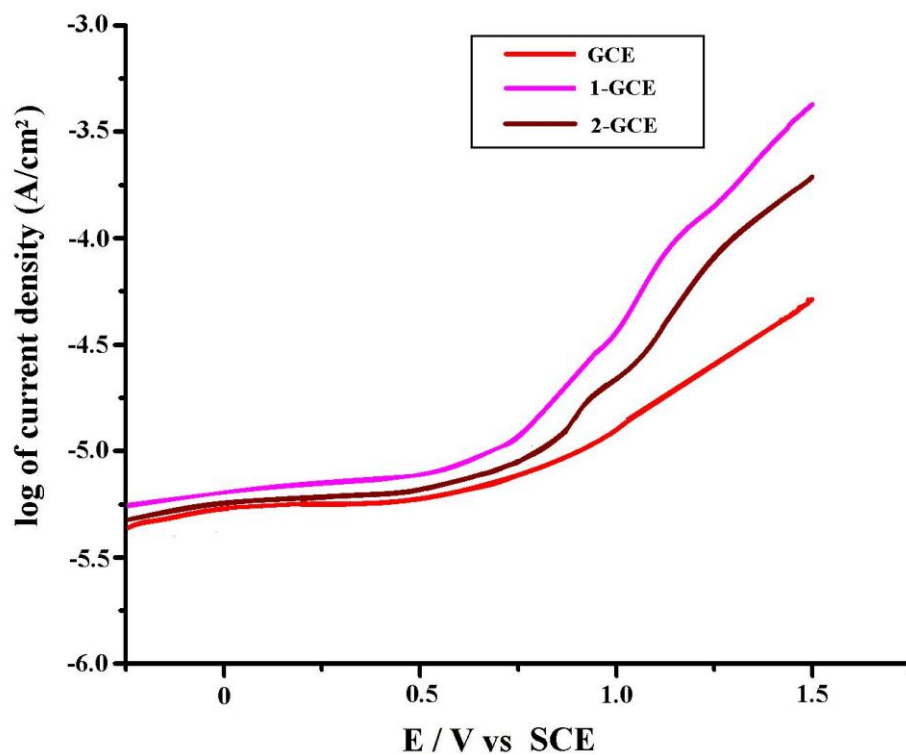
Fig. S6 Tafel plots in the potential range from -0.3 to 1.5 V vs SCE of **1-GCE**, **2-GCE** and the bare **GCE** in aqueous solution buffered to neutral pH by 0.2 M phosphate at sweep rates of 5 mV·s^{-1}.

Fig. S7 Nyquist plots (Z' vs. $-Z''$) of the three-electrode systems in an aqueous solution

buffered to neutral pH (0.2 M phosphate, pH = 6.8) with the bare **GCE, 1-GCE** and

2-GCE as working electrodes, respectively.
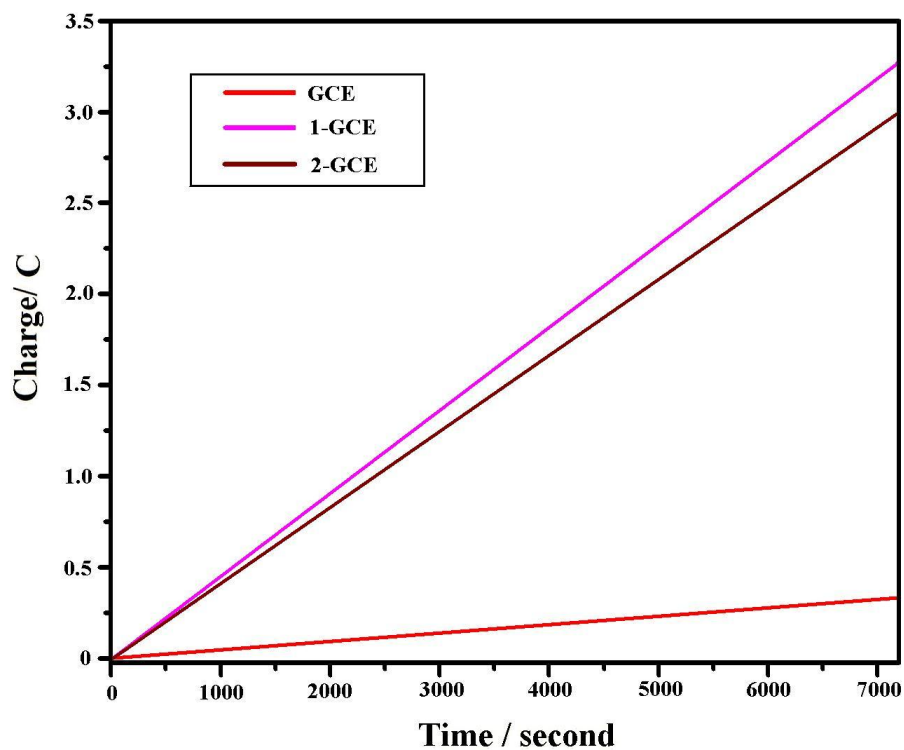
Fig. S8 Controlled potential electrolysis of **1**-**GCE** (current density = 2.32 mA/cm^2), **2**-**GCE** (current density = 2.09 mA/cm^2) and bare **GCE** (current density = 0.25 mA/cm^2) in aqueous solution buffered to neutral pH by 0.2 M phosphate, showing charge buildup versus time with an applied potential of + 1.4 V vs SCE (η = +0.81 V).
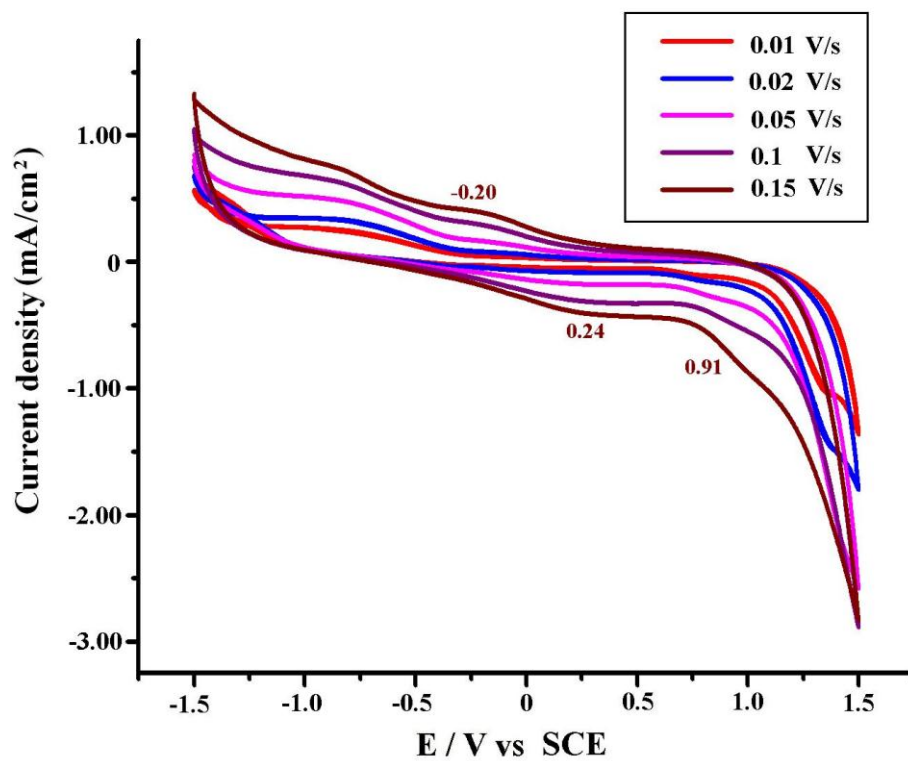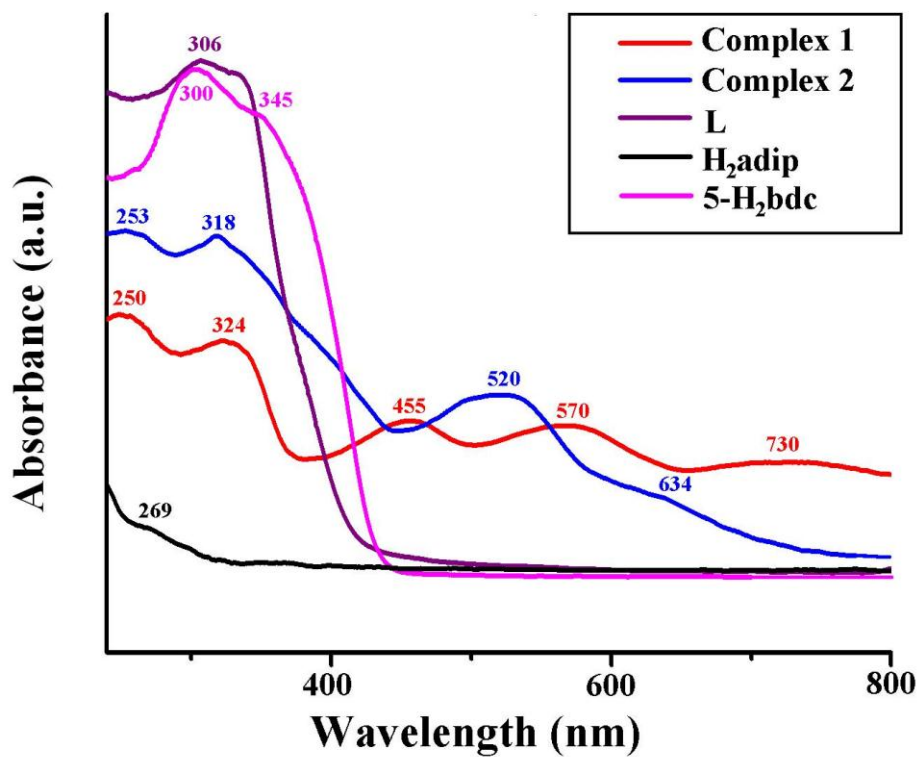
Fig. S9 Cyclic voltammograms of **2-GCE** in an aqueous solution buffered to neutral pH (0.2 M phosphate, pH 6.8) at different sweep rates.
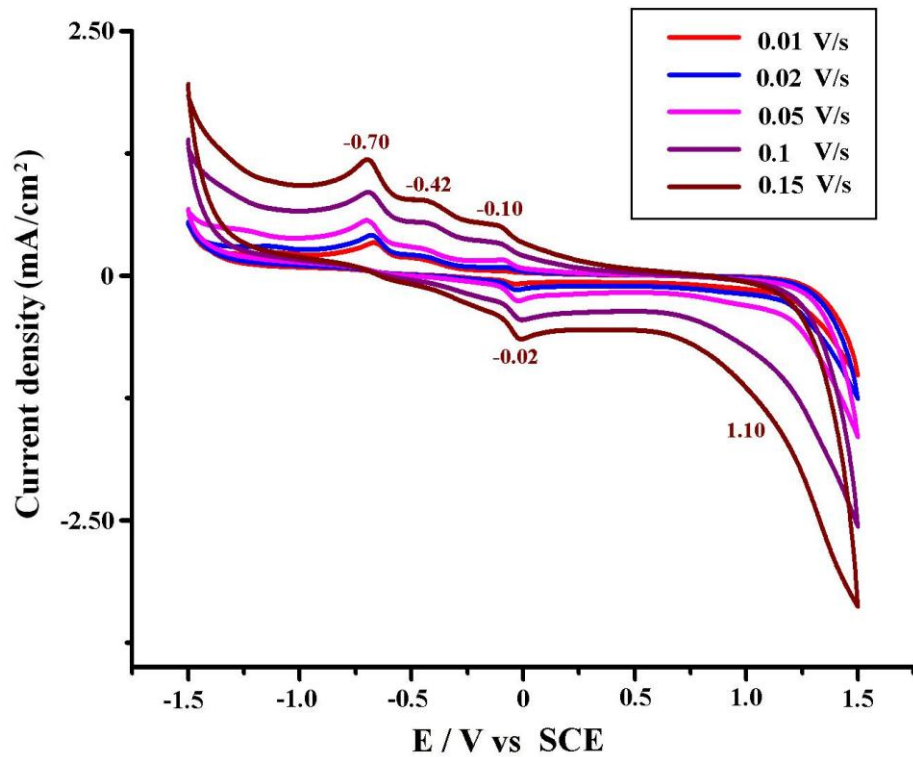
Fig. S10 Cyclic voltammograms of the bare **GCE** in an aqueous solution buffered to neutral pH (0.2 M phosphate, pH = 6.8) containing 4 mg **5-H₂bdc** at different sweep rates.
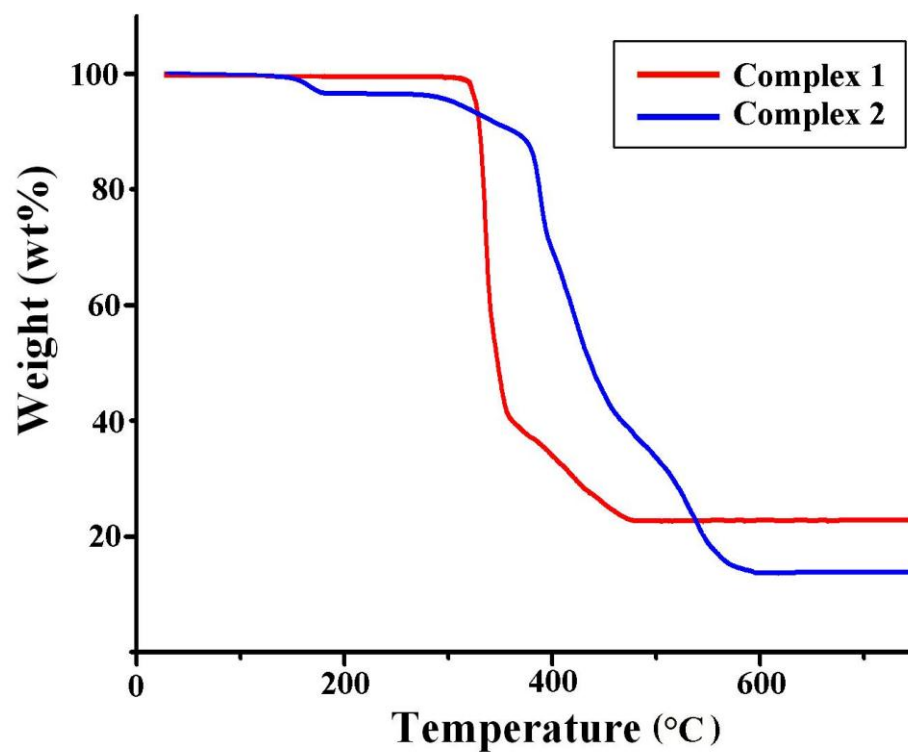
Fig. S11 Thermogravimetric curves of complexes **1** (**red**) and **2** (**blue**).

Fig. S12 UV-vis absorption spectra at room temperature for the free ligands and complexes **1-2**.

Reference:

1 Y. J. Sun, J. P. Bigi, N. A. Piro, M. L. Tang, J. R. Long and C. J. Chang, *J. Am. Chem. Soc.*, **2011**, *133*, 9212.